A Journal of the Gesellschaft Deutscher Chemiker

Angewandte International Edition GDCh Chemie

www.angewandte.org

Accepted Article

Title: Necroptosis Induced by Ruthenium(II) Complexes as Dual Catalytic Inhibitors of Topoisomerase I/II

Authors: Hui Chao, Kai Xiong, Chen Qian, Yixian Yuan, Lin Wei, Xinxing Liao, Liting He, Thomas W. Rees, Yu Chen, Jian Wan, and Liangnian Ji

To be cited as: *Angew. Chem. Int. Ed.* 10.1002/anie.202006089

Link to VoR: https://doi.org/10.1002/anie.202006089

WILEY-VCH

10.1002/anie.202006089

WILEY-VCH

RESEARCH ARTICLE

Necroptosis Induced by Ruthenium(II) Complexes as Dual Catalytic Inhibitors of Topoisomerase I/II

Kai Xiong,[a] Chen Qian,[a] Yixian Yuan,[a] Lin Wei,[b] Xinxing Liao,[a] Liting He,[a] Thomas W. Rees,[a] Yu Chen,*[a] Jian Wan,*[b] Liangnian Ji,[a] and Hui Chao*[a][c]

Abstract: Inducing necroptosis in cancer cells is an effective approach to circumvent drug-resistance. Metal-based triggers have, however, rarely been reported. Ruthenium(II) complexes containing 1,1-(pyrazin-2-yl)pyreno[4,5-e][1,2,4]triazine were developed with a series of different ancillary ligands (**Ru1**-**7**). The combination of the main ligand with bipyridyl and phenylpyridyl ligands endows **Ru7** with superior nucleus-targeting properties. As a rare dual catalytic inhibitor, **Ru7** effectively inhibits the endogenous activities of topoisomerase (topo) I and II and kills cancer cells by necroptosis. The cell signaling pathway from topo inhibition to necroptosis was elucidated. Furthermore, **Ru7** displays significant antitumor activity against drug-resistant cancer cells *in vivo*. To the best of our knowledge, **Ru7** is the first Ru-based necroptosis-inducing chemotherapeutic agent.

Introduction

Cancer drug resistance is a major problem in chemotherapy, which can be caused by the regulation of transporters, up-regulation of detoxification systems or modulation of cell death pathways.[1] Conventional anticancer agents, such as cisplatin, camptothecin, and paclitaxel, mostly induce apoptosis regardless of target and mechanism.[2] It has been demonstrated that many cancer cells exhibit drug resistance *via* dysregulation of apoptotic machinery, including the overexpression of antiapoptotic proteins and defects in apoptotic signalling.[3] As the apoptotic machinery is composed of dozens of antiapoptotic and proapoptotic proteins, which are also affected by many oncogenic signals, it is highly difficult to treat cancers with apoptotic resistance. The apoptotic resistance of cancer cells can, however, be circumvented by chemotherapeutic agents which induce non-apoptotic cell death.[4]

[a] K. Xiong, Dr. C, Qian, Dr. Y. Yuan, X. Liao, L. He, Dr. T. W. Rees, Dr. Y. Chen, Prof. L. Ji and Prof. Dr. H. Chao
MOE Key Laboratory of Bioinorganic and Synthetic Chemistry, School of Chemistry
Sun Yat-Sen University
Guangzhou, 510275, P. R. China
E-mail: chenyu63@mail.sysu.edu.cn, ceschh@mail.sysu.edu.cn
[b] L. Wei, Prof. Dr. J. Wan,
College of Chemistry,
Central China Normal University
Wuhan, 430079, P. R. China
Email: jianwan@mail.ccnu.edu.cn
[c] Prof. Dr. H. Chao
College of Chemistry and Environmental Engineering
Shenzhen University
Shenzhen, 518071, P. R. China

Supporting information for this article is given via a link at the end of the document.

Necrosis was originally considered to be random and unregulated, however, increasing evidence reveals that necrosis can be induced and proceed in a regulated manner like apoptosis. This is known as necroptosis. Necroptosis is intricately connected with many physiological processes and crucial for the maintenance of tissue homeostasis-throughout life.[5] Reports on necroptosis-inducing chemotherapeutic agents are rare, especially metal-based agents. Cisplatin can trigger necrosis in many types of cancer cells. This occurs only in the presence of the caspase inhibitor (Z-VAD-FMK) however, indicating that necroptosis is optimally induced when the apoptotic machinery is compromised.[6] Recently, two rhenium(V) oxo complexes were developed as necroptosis triggers and demonstrated excellent therapeutic efficiency.[7] Zn(II), Ni(II), Os(II), and Fe(III) complexes were also utilized to induce necroptosis in cancer cells.[8] It was noted that cisplatin-induced necroptosis is caspase inhibitor dependent. In contrast, the afore mentioned complexes induce necroptosis in the absence of caspase inhibitors. Although interesting, these complexes need further evaluation of their cellular targets and *in vivo* therapeutic effects. Aside from these few studies, the area remains underexplored.

Topoisomerases (topo) are critical enzymes for the control of DNA supercoiling and entanglement, and are therefore involved in cell proliferation. Topo I and topo II are two types of topoisomerases which are ordinarily over-expressed in tumors.[9] Their respective inhibitors, camptothecin and etoposide, are among the most commonly used anticancer drugs. As is the case for many antitumor drugs, these inhibitors are susceptible to drug resistance. The down-regulation of the targeting enzyme, and

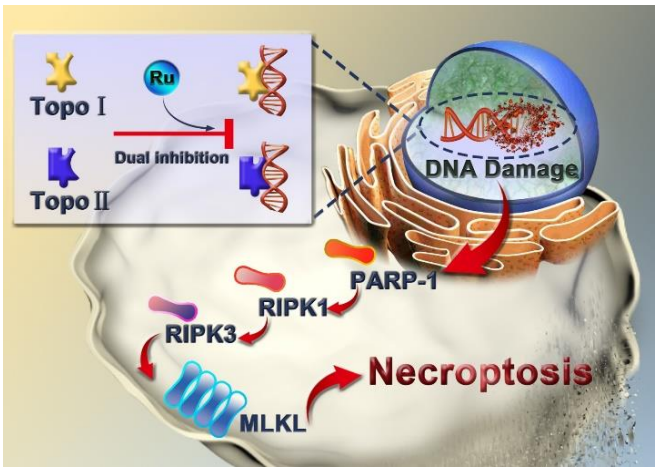

Scheme 1. Schematic illustration of the dual catalytic inhibitor of topoisomerase I and II inducing necroptosis.

10.1002/anie.202006089

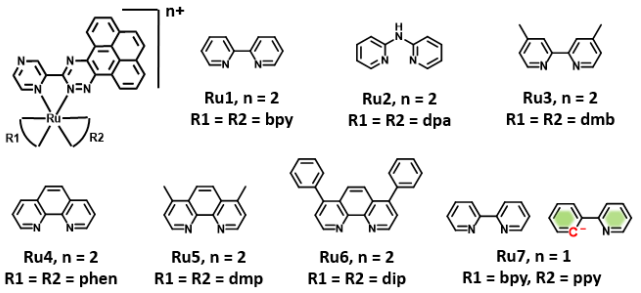

Figure 1. The chemical structures of the Ru(II) complexes **Ru1-7**.

apoptotic machinery dysregulation, are responsible for this.[10] When one of these topoisomerases is suppressed, the other is commensurably overexpressed. Furthermore, simultaneous treatment with the respective inhibitor antagonizes cytotoxic effects.[11] Therefore, simultaneous inhibitors of both topo I and II (dual inhibitors) are expected to have a broader spectrum of activity as expression levels of the two enzymes are variable between different types of cancers and possess a significant therapeutic advantage over agents targeting one type of topoisomerase alone.[12]

Metal complexes have been developed as topo inhibitors and although those reported have displayed remarkable antitumor activity, most of the research so far has focused on either topo I or II alone.[13] Some Ru(II) complexes, such as $[Ru(bpy)_2(pscl)]^{2+}$ and $[Ru(bpy)_2(psbr)]^{2+}$, have been found to efficiently inhibit both topo I and II.[11b] However, they still have several shortcomings: 1) These Ru(II) complexes are all classed as topoisomerase poisons and induce apoptosis. 2) Their nuclear accumulation properties are yet to be confirmed, therefore, the relationship between apoptosis and topo inhibition is in doubt. 3) Their *in vivo* antitumor activity remains uninvestigated. In this context, ruthenium(II) complexes containing 1,1-(pyrazin-2-yl)pyreno[4,5-e][1,2,4]triazine were developed as dual catalytic inhibitors of topo I and topo II (**Ru1**-**7**, Figure 1). The nucleus-targeting of **Ru7** was achieved by adjustment of the auxiliary ligands and thereby the overall properties of the complex. **Ru7** induces necroptosis and the cell signaling pathway involved is herein demonstrated (Scheme 1). The antitumor activity of **Ru7** as the first metal-based topo I/II dual catalytic inhibitor that triggers necroptosis was also evaluated *in vivo*.

Results and Discussion

The main ligand 1,1-(pyrazin-2-yl)pyreno[4,5-e][1,2,4]triazine (pzpp) was obtained in a good yield by the reaction of pyrene-4,5-dione with pyrazine-2-carboxamide hydrazine. Cellular uptake and organelle distribution are a key factor affecting the efficacy of metal-based antitumor agents. Tuning the lipophilicity or charge of a complex is an effective approach to achieve this.[14] With this in mind, auxiliary ligands with increasingly conjugated systems were added to **Ru1**-**6**, while a cyclometalated ligand was introduced to **Ru7**. **Ru1**-**6** were synthesized in a similar manner

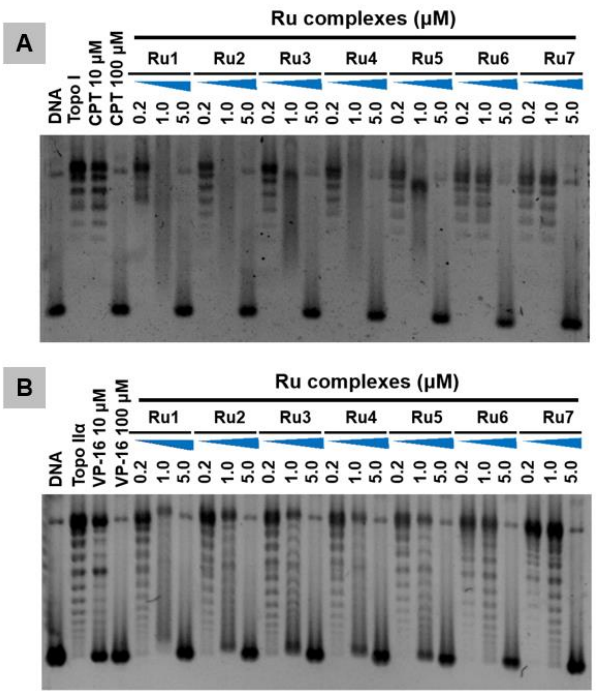

Figure 2. Inhibitory effects of **Ru1**-**7** on the catalytic activity of topoisomerases I (A) and topoisomerase II (B) were determined with relaxation assays.

by heating pzpp with corresponding precursor cis-$Ru(L)_2Cl_2$ [L = 2,2'-bipyridine (bpy, **Ru1**); di(pyridin-2-yl)amine (dpa, **Ru2**); 4,4'-dimethyl-2,2'-bipyridine (dmb. **Ru3**); 1,10-phenanthroline (phen, **Ru4**); 4,7-dimethyl-1,10-phenanthroline (dmp, **Ru5**) and 4,7-diphenyl-1,10-phenanthroline (dip, **Ru6**)] in ethylene glycol at 120 °C for 6 h. For cyclometalated **Ru7**, stoichiometric equivalents of $[(\eta_6\text{-}C_6H_6)Ru(bpy)Cl]$ and 2-phenyl-pyridine (ppy) were combined and refluxed in DMF for 4 h, before the addition of 1 equivalent of pzpp and reflux for further 4 h. All the crude products were purified by chromatography on Al_2O_3 with acetonitrile and toluene mixtures as the eluents. These complexes were fully characterized by elemental analysis, ESI-MS and ^1H NMR spectroscopy (Figure S1-S7). The crystal of **Ru1**, **Ru2**, **Ru3**, **Ru5** and **Ru6** were also obtained by solvent evaporation (acetonitrile and toluene, 1:1, v/v) and the structures determined by single crystal x-ray diffraction. ORTEP representations of the structures including the atom numbering scheme are shown in Figure S8-S12. The X-ray crystallographic data, including selected bond lengths and angles are given in the Supporting Information (Table S1-S6).

The results of Topo I and Topo II inhibition assays with different concentrations of **Ru1**-**7** are shown in Figure 2. **Ru1**-**7** inhibit the ability of topo I and topo II to relax negatively supercoiled plasmid DNA. These results are consistent with known topo I inhibitor camptothecin (CPT) and topo II inhibitor etoposide (VP-16). The inhibition efficacy is concentration-dependent. All the Ru(II) complexes completely inhibit topo I/II activity at a concentration of 5 μM, indicating that their inhibition

10.1002/anie.202006089

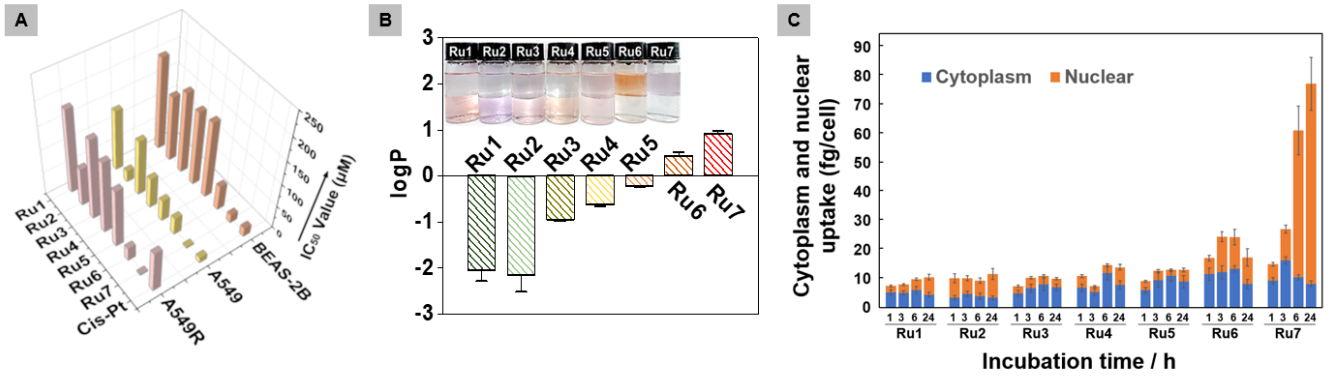

Figure 3. (A) IC_{50} values of cisplatin and **Ru1**-**Ru7** after incubation with the lung cancer cell A549, lung drug-resistant cancer cell A549R and the lung normal cell BEAS-2B for 48 h. (B) The octanol/water partition coefficients of **Ru1**-**Ru7**. Insert: the distributions of **Ru1**-**Ru7** in octanol/water solutions. (C) Amounts of ruthenium within the cytoplasm and nuclei of A549R cells after incubating with **Ru1**-**Ru7** (5 μM) for 1, 3, 6, and 24 h.

abilities are independent of the auxiliary ligand. In contrast, no significant inhibition was observed for 10 μM CPT and VP-16.

Topoisomerase inhibitors are split into two types: poison and catalytic inhibitor.[15] Topoisomerase poisons selectively affect the re-ligation of DNA and form stable enzyme-DNA-inhibitor ternary complexes. Catalytic inhibitors prevent the binding of topo enzymes to DNA. The majority of topo inhibitors are topo poisons and reports on topo I/II dual catalysis inhibitors are rare.[16] This may be due to the structural differences between the two enzymes, resulting in design difficulties.[17] To investigate whether **Ru1**-**7** are topo poisons, the formation of topoisomerase-induced DNA-strand breaks was measured. As shown in Figure S13A, the poison CPT stabilizes the topoisomerase I cleavable complex, resulting in the generation of open-circle plasmid DNA (lane 10, marked with an arrow). In contrast, open-circle DNA bands were not observed for the Ru(II) complexes (lane 3-9), implying the existence of a different inhibition mechanism. Additionally, **Ru1**-**7** antagonize the formation of open-circle DNA in the presence of 20 times higher concentrations of CPT (lane 11-17), suggesting that the Ru(II) complexes act a step upstream of CPT. Similar results were observed for topoisomerase II (Figure S13B). The poison VP-16 selectively affects topo II-mediated DNA re-ligation, which leads to the presence of a linear DNA band. None of the Ru(II) complexes increase the level of DNA scission, but all of them prevent cleavable complex formation in the presence of VP-16, even when the concentration of VP-16 is 20 times that of the complexes.

The ability of **Ru1**-**7** to prevent topoisomerase-DNA binding was studied by electrophoretic mobility shift assay (EMSA).[15b] The results are presented in Figure S14. Topo I forms stable complexes with plasmid DNA, resulting in a relatively immobile band that is retained close to the application slot. Treatment of these complexes with SDS and proteinase K released the DNA. The topo poison CPT did not interfere with the binding and scission steps of topo I. In contrast, topo I binding of DNA was significantly affected by the complexes. A similar result was obtained for topo II. Topo II binds to DNA in both the presence and absence of VP-16, while **Ru1**-**7** prevent this binding. These observations demonstrate that the complexes act as topo I and II dual catalytic inhibitors rather than poisons. This conclusion is further demonstrated by the endogenous topoisomerase inhibition and molecular docking experiments, which follow.

The remarkable topo I and II inhibition properties of **Ru1**-**7** encouraged the investigation of their anticancer activity. Five cancer cell lines (A549, SGC-7091, HeLa, HepG2, and BEL-7402), two drug-resistant cell lines (A549R, and SGC-7901/DDP) and two normal cell lines (LO2, and BEAS-2B) were tested. Cisplatin, CPT, VP-16, and the ligand pzpp were used as controls. The detailed IC_{50} data are shown in Table S7 and the results for A549, A549R, and BEAS-2 are also presented in Figure 3A. The ligand pzpp was inactive against all of the cell lines (IC_{50} > 200 μM). CPT and VP-16 exhibited moderate cytotoxicity towards all the cancer cell lines but much less activity toward normal cells. In contrast, cisplatin showed stronger activity against the cancer cell lines than CPT and VP-16, with the exception of the drug-resistant cell lines. The selectivity of cisplatin between cancer and normal cells is, however, poor. Although **Ru1**-**7** possess similar topoisomerase inhibition abilities, their antitumor activities are varied. **Ru1** and **Ru3** showed the lowest cytotoxicities with IC_{50} > 100 μM. **Ru2**, **Ru4**, and **Ru5** displayed moderate antiproliferative activity similar to CPT. Treatment with **Ru6** inhibited the cancer cells with IC_{50} values in the range of cisplatin. The cyclometalated complex **Ru7** exhibited the most potent anticancer activity. Against A549, for example, the IC_{50} value of **Ru7** is 3.0 ± 0.1 μM, 3.8, 26.3, and 17.5-fold lower than that of cisplatin, CPT, and VP-16, respectively. **Ru7** displayed similar activity towards both the drug-resistant and corresponding cancer cell lines, demonstrating its ability to overcome drug resistance. Moreover, **Ru7** had a high selectivity towards cancer cells over normal cells. The selectivity ratio between normal lung cells BEAS-2B (IC_{50} = 18.0 ± 1.1 μM) and lung cancer cells A549R (IC_{50} = 2.2 ± 0.2 μM) was found to be 8.2. In contrast, the ratios for CPT, VP-16, and cisplatin are 1.4, 2.0, and 0.2, respectively. Although A549 cells are characterized by multidrug resistance *via* P-glycoprotein (transporter) expression rather than reducing apoptosis, A549R cells are more resistant towards cisplatin-induced apoptosis than SGC-7901/DDP. Therefore, the following experiments were performed in A549R cells.

10.1002/anie.202006089

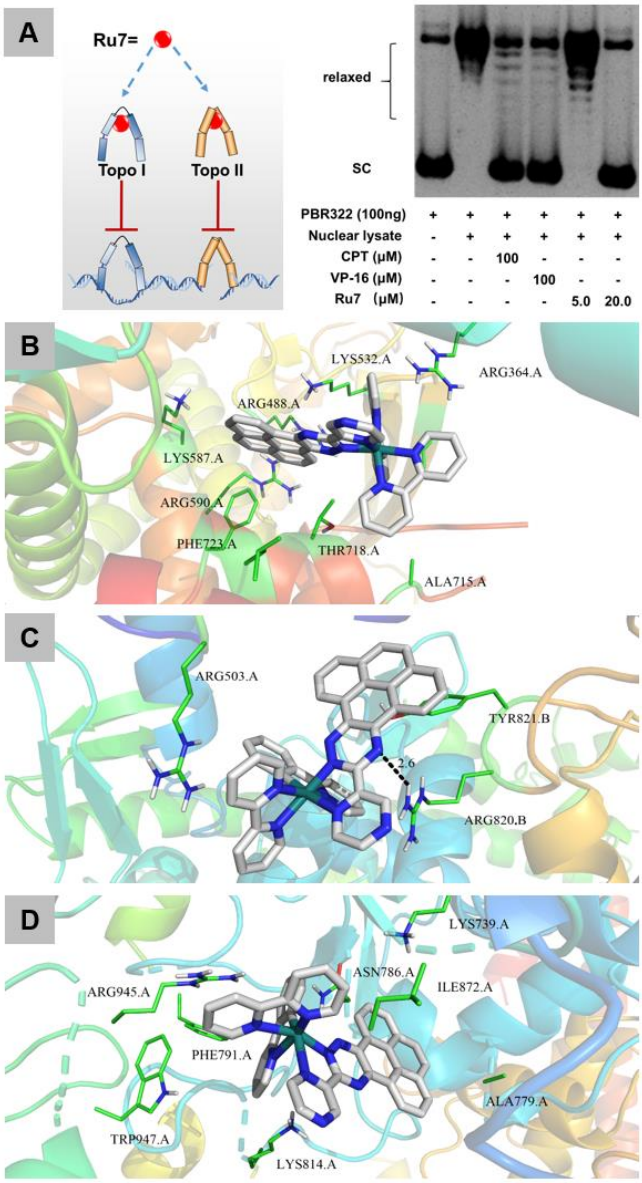

Figure 4. (A) Left: schematic illustration of the dual catalytic inhibition mechanism. Right: endogenous topo inhibition assay. A549R cells were pretreated with CPT, VP-16, or **Ru7** for 24 h and then the nuclear lysates were incubated with 100 ng of pBR322 plasmid at 37 °C for 30 min. (B) Molecular docking experiments indicate that **Ru7** can bind to the DNA-binding site of topoisomerase I. (C-D) Molecular docking results for the interations between **Ru7** and the topoisomerase II DNA-binding site (C) and ATP-binding site (D).

The cellular uptake and organelle localization of the complexes was investigated in order to determine the cause of variation in cytotoxicity across the series. The ability of Ru(II) complexes to pass through cell membranes is related to their lipophilicity. The octanol/water partition coefficients (log $P_{O/W}$) of the complexes were therefore assessed.[18] As expected, the lipophilicities of **Ru1**-**6** increase with the degree of conjugation of the auxiliary ligands. **Ru1**-**5** are hydrophilic while **Ru6** and **Ru7** are lipophilic. **Ru2,** with the imino group, showed the most negative log $P_{O/W}$ value (-2.15 ± 0.36). Replacing the auxiliary bipyridyl ligand (**Ru1**) with phenanthroline (**Ru4**), gave an increase in log $P_{O/W}$ value from -2.06 ± 0.23 to -0.62 ± 0.04. Further addition of methyl groups (**Ru5**, -0.22 ± 0.02) and phenyl groups (**Ru6**, 0.43 ± 0.07) also increased the lipophilicity. The cyclometalated complex **Ru7** with a charge of +1 compared with the +2 charge of the other complexes has the highest lipophilicity of the series, which is predictive of a higher cellular uptake (Figure 3B). To achieve topoisomerase inhibition, localization in the cell's nucleus is necessary. The nucleus-targeting properties of the complexes were investigated by inductively coupled plasma mass spectrometry (ICP-MS). The ICP-MS data match the trends observed in lipophilicity and antitumor activity experiments (Figure 3C). The cellular uptakes of **Ru1-5** were poor. Containing the lipophilic ligand dip, the cellular uptake of **Ru6** was significantly higher than those of **Ru1-5**. Although the nucleus-localized amount of **Ru6** was also increased, its cytosolic fraction was still up to 52.3% (24 h). In contrast, the cyclometalated complex **Ru7** displayed the most potent nuclear-targeting activity. After 24 h incubation, the nuclear fraction is 89.2%, confirming its specific nuclear-targeting property. Due to its optimal antitumor activity and selectivity, **Ru7** was chosen for further studies in A549R cells.

To further confirm the nuclear localization of **Ru7** and verify whether **Ru7** can inhibit topoisomerases in cells, a cell-based DNA relaxation assay was performed. A549R cells were treated with **Ru7** for 24 h and the nucleus was extracted. The nuclear extractions were lysis and used for the assay.[12b] If **Ru7** cannot enter the nucleus nor inhibit the topoisomerases, the result for **Ru7**-treated and **Ru7**-free samples will be the same, that is, the topoisomerases keep active. As shown in Figure 4A, in the absence of **Ru7**, the endogenous topoisomerases in the nuclear lysates made the supercoiled plasmids completely relaxed or linearized (lane 2). Incubation with 100 μM CPT or VP-16 inhibited the endogenous topoisomerases due to the formation of stable enzyme-DNA-inhibitor complexes. Low concentration treatment with **Ru7** (5 μM) did not affect the topo-mediated relaxation. When the concentration was increased to 20 μM, a strong inhibition was observed (lane 6). Because the above cleavable complex assay demonstrated that the Ru(II) complexes are topo I and II dual catalytic inhibitors, this endogenous topo inhibition was assigned to the binding of **Ru7** to topo I and topo II. Molecular docking experiments were performed to provide insight into the mode of action of **Ru7** as a topo catalytic inhibitor. With topo I, **Ru7** is predicted to bind to the DNA-binding pocket (Figure 4B). π-π stacking between **Ru7** and PHE723, ARG364, ARG488, and ARG590, as well as the cation-π interaction with LYS532 accounts for the inhibition. Results with topo II show that there are two potential binding modes for **Ru7**. The first one is similar to the case of topo I. **Ru7** could localize in the DNA-binding pocket of topo II through hydrogen bonding with ARG820, and π-π stacking with ARG503 and TYR821 (Figure 4C). As the activation of topo II requires ATP, **Ru7** could also bind to the ATP pocket of topo II (Figure 4D), stabilized *via* π-π stacking (with PHE791, ARG945, ARG488, and TRP947) and cation-π interactions (with LYS814 and LYS739).

The mechanism of cell death induced by **Ru7** was evaluated next. The cytotoxicity of **Ru7** in the presence of inhibitors was studied. A549R cells were pretreated for 0.5 h with Z-VAD-FMK

10.1002/anie.202006089

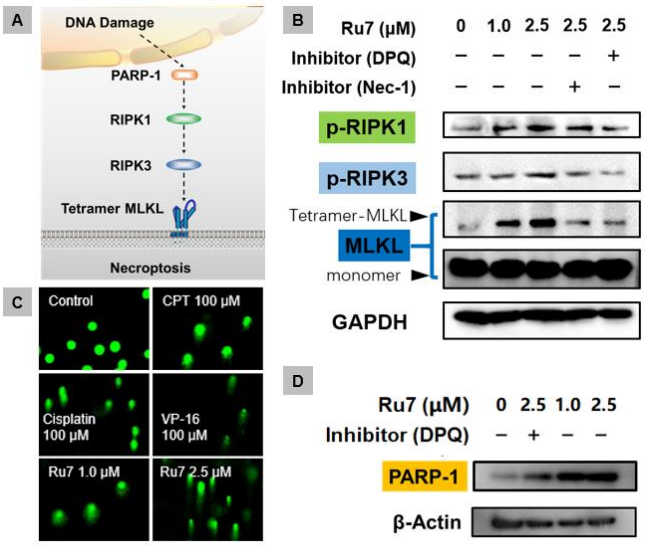

Figure 5. (A) The cell signaling pathway from topo inhibition to necroptosis. (B) The expression level of phospho-RIPK1 (p-RIPK1), phospho-RIPK3 (p-RIPK3), and MLKL with or without the presence of inhibitors (DPQ, PARP-1 inhibitor; Nec-1, RIPK1 inhibitor). (C) Nuclear DNA damage was examined by the comet assay. (D) The expression level of PARP-1 with or without the presence of inhibitor DPQ.

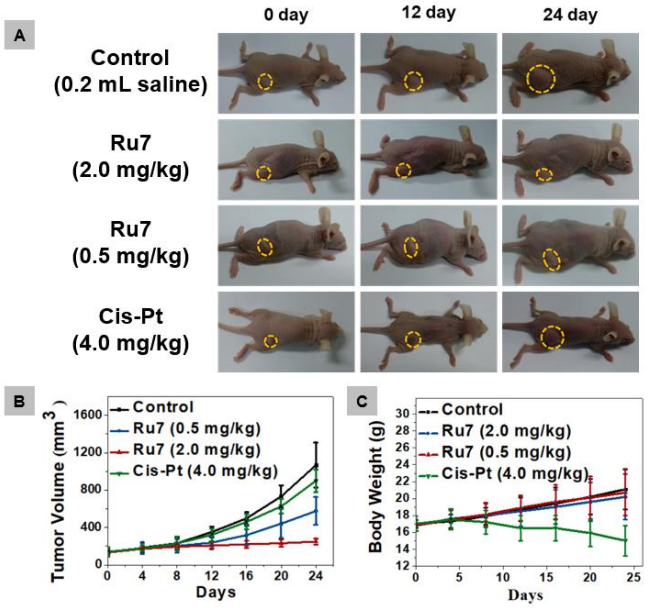

Figure 6. The *in vivo* antitumor activity of **Ru7** towards A549R xenografted tumor. (A) Representative photographs of mice after treatments with saline (0.2 mL, Control), **Ru7 (**high dose, 2.0 mg/kg), **Ru7** (low dose, 0.5 mg/kg) and cisplatin (4.0 mg/kg, Cis-Pt). Tumor volumes (B) and body weights (C) change curves of various treatments as indicated. The error bars denote the standard deviation of results from ten mice.

(apoptosis inhibitor), 3-methyladenine (autophagy inhibitor) and necrostatin-1 (necrosis and necroptosis inhibitor) followed by **Ru7** (2.5 μM) for a further 24 h.[19] As shown in Figure S15, with addition of Z-VAD-FMK, no effect on the cell survival rate was observed (cell viability = 70.1%) when compared with treatment **Ru7** alone (cell viability = 68.1%), indicating that apoptosis was not involved in the cell death pathway induced by **Ru7**. this was further demonstrated by caspase activation assay. Caspase is an important protein family involved in apoptosis. As expected, caspases were activated in response to cisplatin while treatment with **Ru7** antagonized activation (Figure S16). Similarly, autophagy was not found to be involved in **Ru7** induced cell death as the presence of autophagy inhibitor 3-methyladenine did not affect the cell survival rate (Figure S15) and no activation of LC3 was observed (Figure S17). In contrast, **Ru7** driven cell death was significantly reduced in the presence of necrostatin-1 (cell viability = 90.5%, *t* test, $p < 0.05$). The cell death mechanism was further investigated by Annexin V-FITC/propidium iodide (AV/PI) dual staining assay (Figure S18). The results show that cisplatin, CPT, and VP-16 treatment leads to increase in the number of AV^+PI^- cells with a constant percentage of AV^-PI^+ cells. This results from the externalization of phosphatidyl-serine on the cell surface, an early indicator of apoptosis. Significantly different phenomena were observed on treatment with **Ru7** (1 μM). 19.5% of cells were permeable to PI while that for control was 6.2%. Although the percentage of AV^+PI^- cells increased slightly from 3.9% to 7.5%, it did not increase further when the concentration of **Ru7** was increased to 2.5 μM. In contrast, 2.5 μM **Ru7**-treatment remarkably increased the percentage of AV^-PI^+ cells, with severely damaged plasma membranes. This result, together with the above cytotoxicity results, demonstrate that **Ru7** induces necrosis or necroptosis

The main difference between necrosis and necroptosis is that the latter is regulated. The core necroptotic pathway is receptor-interacting protein kinase 1 (RIPK1)–RIPK3–mixed lineage kinase domain-like protein (MLKL) (Figure 5A).[20] The immunoblotting results in Figure 5B show that with **Ru7** treatment, the expression of phospho-RIPK1 (p-RIPK1), phospho-RIPK3 (p-RIPK3), tetramer-MLKL increased while the amount of mono-MLKL was reduced in a concentration-dependent manner. This activation could be blocked by the presence of RIPK1 inhibitor necrostatin-1 (Nec-1),[13c] which is consistent with the above cytotoxicity result (Figure S15). Upstream of RIPK1 and its relationship with topo inhibition were also determined. Recent reports have linked the activation of poly(ADP-ribose) polymerase (PARP-1) to the expression of RIPK1.[21] As a DNA repair enzyme, PARP-1 can be triggered by DNA damage.[13c,22] Nuclear DNA damage was therefore examined by a comet assay (Figure 5C). Treatment with **Ru7** led to the appearance of a “broom-like” tail indicating severe DNA damage. This result was consistent with that of cisplatin, CPT, VP-16, and previously reported topo catalytic inhibitors.[23] Subsequent activation of PARP-1 was similar to that of p-RIPK1, p-RIPK3 and tetramer-MLKL (Figure 5D). Co-incubation with 3, 4-Dihydro-5[4-(1-piperindinyl)butoxy]-1(2H)-isoquinoline (DPQ), a selective PARP-1 inhibitor, not only inhibited the expression of p-RIPK1, p-RIPK3 and tetramer-MLKL (Figure 5B) but also markedly decreased the cytotoxicity of **Ru7** (Figure S15), confirming that PARP-1 acts as the upstream of the necroptotic pathway and is involved in **Ru7**-induced cell death. In addition, it has been reported that the RIP1-RIP3-MLKL complex mediates downstream executing molecules and events such as reactive oxygen species (ROS) burst, plasma membrane permeabilization and cytosolic ATP reduction. ROS levels were

measured by staining with DCFH-DA and ATP levels were examined by luciferase assay. As shown in Figure S19, after incubation with **Ru7**, enhancement of cellular ROS production and decrease in ATP levels were observed. Plasma membrane permeabilization was assessed by lactate dehydrogenase (LDH) release. A 2.0 and 3.3-fold increase in the luminescence intensity of released LDH was obtained after 1 and 2.5 μM **Ru7** treatments respectively (Figure S19).

As the *in vivo* antitumor activity of metal-based necroptosis inducers remains an unexplored area of research, the *in vivo* antitumor activity of **Ru7** was evaluated. A549R xenografted tumor-bearing mice were randomly divided into four groups, named control (0.2 mL saline), high dose (**Ru7**, 2.0 mg/kg), low dose (**Ru7**, 0.5 mg/kg) and Cis-Pt (cisplatin, 4.0 mg/kg). Intraperitoneal injections were given every 4 days to all groups. As shown in Figure 6, the cisplatin treated group showed similar tumor development to the control due to the cisplatin resistance of the cell line. In contrast, **Ru7** significantly inhibited tumor development. After 24 days of treatment, the tumor growth of the high dose group was negligible, and the average volume was only 23.3% of that of the control group. Furthermore, the body weights of all groups, except cisplatin, increased in a stable manner during treatment (Figure 6) with no serious cellular structural changes, pathological alterations or organ damage observed (Figure S20). In contrast, the cisplatin treated group exhibited significant loss of body weight and evident liver and kidney damage. These results confirm the advantages of **Ru7** as a necroptotic inducer for the treatment of drug resistant cancer.

Conclusion

In this work, ruthenium(II) complexes, **Ru1**-**7**, were developed as chemotherapeutic agents. **Ru1**-**7** are highly novel catalytic inhibitors of both topoisomerase I and II preventing the topoisomerases from binding to DNA. The antitumor activities of **Ru1**-**7** vary with lipophilicity, resulting from differences in cellular uptake. Introduction of the cyclometalated auxiliary ligand to **Ru7** endows the complex with excellent nucleus-targeting properties. **Ru7** displays remarkable cytotoxicity against various cancer cell lines including cisplatin-resistant cancer cells, demonstrating the complexes ability to overcome drug resistance. Furthermore, the cytotoxicity of the complex is highly selective towards cancer cells over normal cell lines. Screening with inhibitors of different cell death modes revealed **Ru7** induces necroptosis. Characteristic indicators of necroptosis were observed, including ROS burst, plasma membrane permeabilization and cytosolic ATP reduction. The cell signalling pathway from topo inhibition to necroptosis was also demonstrated. **Ru7** inhibits topo I and II, leading to DNA damage and PARP-1 activation, subsequent RIPK1, RIPK3, and MLKL activation results in necroptosis. Finally, the excellent *in vivo* antitumor activity of the complexes was demonstrated proving **Ru7** is a necroptosis-inducing chemotherapeutic agent with great clinical potential for circumventing drug resistance in cancer. We hope that our results will provide new evidence that the induction of necroptosis in cancer cells is an effective way to circumvent drug resistance, and hopefully, in the future, necroptosis inducers can be applied in the clinic treatment.

Experimental Section

Experimental details including synthetic details, characterization data, experimental data and analysis are provided in the Supporting Information. Single-crystal X-ray structure CCDC deposition codes: **Ru1**, 1941708; **Ru2**, 1941709; **Ru3**, 1941706; **Ru5**, 1941707 and **Ru6**, 1941705

Acknowledgements

This work was supported by the National Science Foundation of China (Nos. 21525105, 21778079, 21977126), the Ministry of Education of China (No. IRT-17R111), the Fundamental Research Funds for the Central Universities (No. 20lgjc01), and the Pearl River S&T Nova Program of Guangzhou (No. 201806010136).

Keywords: Bioinorganic Chemistry • Medicinal Inorganic Chemistry • Metals in Medicine • Ruthenium • Necroptosis

[1] a) N. Vasan, J. Baselga, D. M. Hyman, *Nature* **2019**, *575*, 299-309; b) R. W. Robey, K. M. Pluchino, M. D. Hall, A. T. Fojo, S. E. Bates, M, M. Gottesman, *Nat. Rev. Cancer* **2018**, *18*, 452-464; c) X. Wang, X. Wang, S. Jin, N. Muhammad, Z. Guo, *Chem. Rev.* **2019**, *119*, 1138-1192; d) C. Kunick, I. Ott, *Angew. Chem. Int. Ed.* **2010**, *49*, 5226-5227; d)

[2] a) R. G. Kenny, C. J. Marmion, *Chem. Rev.* **2019**, *119*, 1058-1137; b) J. J. Wilson, S. J. Lippard, *Chem. Rev.* **2014**, *114*, 4470-4495; c) A. R. Simović, R. Masnikosa, I. Bratsos, E. Alessio, *Coord. Chem. Rev.* **2019**, *398*, 113011; d) J. P. Gillet, A. M. Calcagno, S. Varma, M. Marino, L. J. Green, M. I. Vora, C. Patel, J. N. Orina, T. A. Eliseeva, V. Singal, R. Padmanabhan, B. Davidson, R. Ganapathi, A. K. Sood, B. R. Rueda, S. V. Ambudkar, M. M. Gottesman, *Proc. Nati. Acad. Sci. USA.* **2011**, *108*, 18708-18713.

[3] a) B. Englinger, C. Pirker, P. Heffeter, A. Terenzi, C. R. Kowol, B. K. Keppler, W. Berger, *Chem. Rev.* **2019**, *119*, 2, 1519-1624; b) T. R. Wilson, P. G. Johnston, D. B. Longley, *Curr. Cancer Drug Tar.* **2009**, *9*, 307-319; c) C. Holohan, S. V. Schaeybroeck, D. B. Longley, P. G. Johnston, *Nat. Rev. Cancer* **2013**, *13*, 714-726; d) K. Liu, L. Gao, X. Ma, J. J. Huang, J. Chen, L. Zeng, C. R. Ashby Jr. C. Zou, Z. S. Chen, *Mol. Cancer* **2020**, *19*, 54.

[4] a) W. Han, L. Li, S. Qiu, Q. Lu, Q. Pan, Y. Gu, J. Luo, X. Hu, *Mol. Cancer Ther.* **2007**, *6*, 1641-1649; b) K. Wang, C. Zhu, Y. He, Z. Zhang, W. Zhou, N. Muhammad, Y. Guo, X. Wang, Z. Guo, *Angew. Chem. Int. Ed.* **2019**, *58*, 4638-4643; c) C. Li, K. W. Ip, W. L. Man, D. Song, M. L. He, S. M. Yiu, T. C. Lau, G. Zhu, *Chem. Sci.* **2017**, *8*, 6865-6870; d) C. Imberti, P. Zhang, H. Huang, P. J. Sadler, *Angew. Chem. Int. Ed.* **2019**, *59*, 61-73; e) Z. Deng, N. Wang, Y. Liu, Z. Xu, Z. Wang, T. Lau, G. Zhu, *J. Am. Chem. Soc.* **2018**, 3426; f) K. N. de Oliveira, V. Andermark, L. A. Onambele, G. Dahl, A. Prokop, I. Ott, *Eur. J. Med. Chem.* **2014**, *87*, 794-800; g) D. Y. Q. Wong, W. W. F. Ong, W. H. Ang, *Angew. Chem. Int. Ed.* **2015**, *54*, 6483-6487.

[5] a) M. Pasparakis, P. Vandenabeele, *Nature* **2015**, *517*, 311-320; b) P. Vandenabeele, L. Galluzzi, T. V. Berghe, G. Kroemer, *Nat. Rev. Mol. Cell Biol.* **2010**, *11*, 700-714; c) A. Linkermann, D. R. Green, *N. Engl. J. Med.* **2014**, *370*, 455-465.

[6] M. J. Choi, H. Kang, Y. Y. Lee, O. S. Choo, J. H. Jang, S. H. Park, J. S. Moon, S. J. Choi, Y. H. Choung, *Cells* **2019**, *8*, 409-; b) Z Su, Z Yang, L Xie, J. P. DeWitt, Y. Chen, *Cell Death Differ.* **2016**, *23*, 748-756.

[7] K. Suntharalingam, S. G. Awuah, P. M. Bruno, T. C. Johnstone, F. Wang, W. Lin, Y. R. Zheng, J. E. Page, M. T. Hemann, S. J. Lippard, *J. Am. Chem. Soc.* **2015**, *137*, 2967−2974.

[8] a) M. Zec, T. Srdić-Rajić, A. Krivokuća, R. Janković, T. Todorović, K. Anđelković, S. Radulović, *Med. Chem.* **2014**, *10*, 759-771; b) M. Flamme,

P. B. Cressey, C. Lu, P. M. Bruno, A. Eskandari, M. T. Hemann, G. Hogarth, K. Suntharalingam, *Chem. Eur. J.* **2017**, *23*, 9674-9682; c) V. Novohradsky, L. Markova, H. Kostrhunova, Z. Trávníček, V. Brabec, J. Kasparkova, *Sci Rep.* **2019**, *9*, 13327; d) J. Sagasser, B. N. Ma, D. Baecker, S. Salcher, M. Hermann, J. Lamprecht, S. Angerer, P. Obexer, B. Kircher, R. Gust, *J. Med. Chem.* **2019**, *62*, 8053−8061.

[9] a) Y. Pommier, *Nat. Rev. Cancer* **2006**, *6*, 789-802; b) J. L. Nitiss, *Nat. Rev. Cancer* **2009**, *9*, 338-350.

[10] a) A. Saleem, T. K. Edwards, Z. Rasheed, E. H. Rubin, *Ann. N. Y. Acad. Sci.* **2000**, *922*, 46-55; b) M. H. Lawson, N. M. Cummings, D. M. Rassl, R. Russell, J. D. Brenton, R. C. Rintoul, G. Murphy, *Cancer Res.* **2011**, *71*, 4877-4887.

[11] a) R. Kim, N. Hirabayashi, M. Nishiyama, K. Jinushi, T. Toge, K. Okada, *Int. J. Cancer* **1992**, *50*, 760-766; b) Y. C. Wang, C. Qian, Z. L. Peng, X. J. Hou, L. L, Wang, H. Chao, L. N. Ji, *J. Inorg. Biochem.* **2014**, *130*, 15-27.

[12] a) V. A. Rao, K. Agama, S. Holbeck, Y. Pommier, *Cancer Res.* **2007**, *67*, 9971–9979; b) H. B. Kwon, C. Park, K. H. Jeon, E. Lee, S. E. Park, K. Y. Jun, T. M. Kadayat, P. Thapa, R. Karki, Y. Na, M. S. Park, S. B. Rho, E. S. Lee, Y. Kwon, *J. Med. Chem.* **2015**, *58*, 1100-1122.

[13] a) V. Brabec, J. Kasparkova, *Coord. Chem. Rev.* **2018**, *376*, 75-94; b) A. Notaro, G. Gasser, *Chem. Soc. Rev.* **2017**, *46*, 7317-7337; c) K. J. Akerman, A. M. Fagenson, V. Cyril, M. Taylor, M. T. Muller, M. P. Akerman, O. Q. Munro, *J. Am. Chem. Soc.* **2014**, *136*, 5670-5682; d) C. G. Oliveira, I. Romero-Canelón, M. M. Silva, J. P. C. Coverdale, P. I. S. Maia, A. A. Batista, S. Castelli, A. Desideri, P. J. Sadler, V. M. Deflon, *Dalton Trans.* **2019**, *48*, 16509-16517; e) S. Movassaghi, E. Leung, M. Hanif, B. Y. T. Lee, H. U. Holtkamp, J. K. Y. Tu, T. Söhnel, S. M. F. Jamieson, C. G. Hartinger, *Inorg. Chem.* **2018**, *57*, 8521-8529.

[14] a) L. Oehninger, S. Spreckelmeyer, P. Holenya, S. M. Meier, S. Can, H. Alborzinia, J. Schur, B. K. Keppler, St. Wölfl, I. Ott*, J. Med. Chem.* **2015**, *58*, 9591−9600; b) W. X. Ni, W. L. Man, S. M. Yiu, M. Ho, M. T. W. Cheung, C. C. Ko, C. M. Che, Y. W. Lam, T. C. Lau, *Chem. Sci.* **2012**, *3*, 1582-1588; c) J. Karges, F. Heinemann, M. Jakubaszek, F. Maschietto, C. Subecz, M. Dotou, R. Vinck, O. Blacque, M. Tharaud, B. Goud, E. V. Zahínos, B. Spingler, I. Ciofini, G. Gasser, *J. Am. Chem. Soc.* **2020**, 6066; d) D. Truong, M. P. Sullivan, K. K. H. Tong, T. R. Steel, A. Prause, J. H. Lovett, J. W. Andersen, S. M.F. Jamieson, H. H. Harris, I. Ott, C. M. Weekley, K. Hummitzsch, T. Söhnel, M. Hanif, N. Metzler-Nolte, D. C. Goldstone, C. G. Hartinger, *Inorg. Chem.* **2020**, *59*, 3281-3289.

[15] a) B. L. Yao, Y. W. Mai, S. B. Chen, H. T. Xie, P. F. Yao, T. M. Ou, J. H. Tan, H. G. Wang, D. Li, S. L. Huang, L. Q. Gu, Z. S. Huang, *Eur. J. Med. Chem.* **2015**, *92*, 540-553; b) T. Syrovets, B. Buchele, E. Gedig, J. R. Slupsky, T. Simmet, *Mol. Pharmacol.* **2000**, 58, 71-81.

[16] a) Y. Pommier, *ACS Chem. Biol.* **2013**, *8*, 82-95; b) B. Kundu, S. K. Das, S. P. Chowdhuri, S. Pal, D. Sarkar, A. Ghosh, A. Mukherjee, D. Bhattacharya, B. B. Das, A. Talukdar, *J. Med. Chem.* **2019**, *62*, 3428-3446.

[17] a) C. Bailly, *Chem. Rev.* **2012**, *112*, 3611-3640; b) S. M. V. de Almeida, A. G. Ribeiro, G. C. de L. Silva, J. E. F. Alves, E. I. C. Beltrão, J. F. de Oliveira, L. B. de Carvalho, M. do C. A. de Lima, *Biomed. Pharmacother.* **2017**, *96*, 1538-1556.

[18] a) S. R. McWhinney, R. M. Goldberg, H. L. McLeod, *Mol. Cancer Ther.* **2009**, 8, 10-16; b) H. Huang, P. Zhang, H. Chen, L. Ji, H. Chao, *Chem. Eur. J.* **2015**, *21*, 715-725; c) S. M. Meier-Menches, C. Gerner, W. Berger, C. G. Hartinger, B. K. Keppler, *Chem. Soc. Rev.* **2018**, *47*, 909-928.

[19] a) R. Guan, Y. Chen, L. Zeng, T. W. Rees, C. Jin, J. Huang, Z. S. Chen, L. Ji, H. Chao, *Chem. Sci.* **2018**, *9*, 5183-5190; b) K. M. Knopf, B. L. Murphy, S. N. MacMillan, J. M. Baskin, M. P. Barr, E. Boros, J. J. Wilson, *J. Am. Chem. Soc.* **2017**, 139, 14302-14314; c) C. Ouyang, L. Chen, T. W. Rees, Y. Chen, J. Liu, L. Ji, J. Long, H. Chao, *Chem. Commun.* **2018**, *54*, 6268-6271.

[20] a) D. Chen, J. Yu, L. Zhang, *BBA-Rev. Cancer* **2016**, *1865*, 228-236; b) Z. Su, Z. Yang, Y. Xu, Y. Chen, Q. Yu, *Mol. Cancer* **2015**, *14*, 48.

[21] a) J. Sosna, S. Voigt, S. Mathieu, A. Lange, L. Thon, P. Davarnia, T. Herdegen, A. Linkermann, A. Rittger, F. K. Chan, D. Kabelitz, S. Schutze, D. Adam, *Cell. Mol. Life Sci.* **2014**, 71, 331-348; b) F. Aredia, A. I. Scovassi, *Biochem. Pharmacol.* **2014**, *92*, 157-163.

[22] a) H. Huang, K. Cao, Y. Kong, S. Yuan, H. K. Liu, Y. Wang, Y. Liu, *Chem. Sci.* **2019**, *10,* 9721-9728; b) X. Xue, C. Qian, H. Fang. H. K. Liu, H. Yuan, Z. Guo, Y. Bai, W. He, *Angew. Chem. Int. Ed.* **2019**, 58, 12661-12666.

[23] a) K. H. Jeon, C. Park, T. M. Kadayat, A. Shrestha, E. S. Leeb, Y. Kwon, *Chem. Commun.* **2017**, *53*, 6864-6867; b) L. Wang, D. A. Eastmond, *Environ. Mol. Mutagen.* **2002**, *39*, 348-356.

10.1002/anie.202006089

WILEY-VCH

RESEARCH ARTICLE

Entry for the Table of Contents (Please choose one layout)

Layout 1:

RESEARCH ARTICLE

Ru(II) complexes were developed to act as dual catalytic inhibitors of topoisomerase I and II. Tuning of the auxiliary ligands gave complex **Ru7**, which targets the nucleus of cancer cells effectively, inducing cell death *via* necroptosis. The cell signaling pathways were investigated and the *in vivo* activity against drug resistant cancer was found to be excellent.

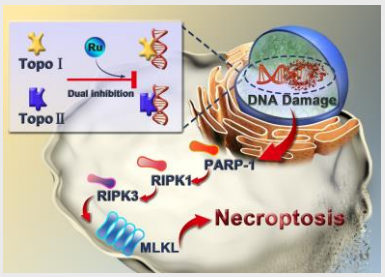

Kai Xiong, Chen Qian, Yixian Yuan, Lin Wei, Xinxing Liao, Liting He, Thomas W. Rees, Yu Chen, Jian Wan,* Liangnian Ji and Hui Chao**

Page No. – Page No.

Necroptosis Induced by Ruthenium(II) Complexes as Dual Catalytic Inhibitors of Topoisomerase I/II

Layout 2:

RESEARCH ARTICLE

((Insert TOC Graphic here))

*Author(s), Corresponding Author(s)**

Page No. – Page No.

Title

Text for Table of Contents